World Academy of Science, Engineering and Technology
International Journal of Materials and Metallurgical Engineering
Vol:10, No:5, 2016

Influence of Iron Ore Mineralogy on Cluster Formation inside the Shaft Furnace

M. Bahgat, H. A. Hanafy, S. Lakdawala

***Abstract*—**Clustering phenomenon of pellets was observed frequently in shaft processes operating at higher temperatures. Clustering is a result of the growth of fibrous iron precipitates (iron whiskers) that become hooked to each other and finally become crystallized during the initial stages of metallization. If the pellet clustering is pronounced, sometimes leads to blocking inside the furnace and forced shutdown takes place. This work clarifies further the relation between metallic iron whisker growth and iron ore mineralogy. Various pellet sizes (6 – 12.0 & +12.0 mm) from three different ores (A, B & C) were (completely and partially) reduced at 985 ^{o}C with H_2/CO gas mixture using thermos-gravimetric technique. It was found that reducibility increases by decreasing the iron ore pellet's size. Ore (A) has the highest reducibility than ore (B) and ore (C). Increasing the iron ore pellet's size leads to increase the probability of metallic iron whisker formation. Ore (A) has the highest tendency for metallic iron whisker formation than ore (B) and ore (C). The reduction reactions for all iron ores A, B and C are mainly controlled by diffusion reaction mechanism.

***Keywords*—**Shaft furnace, cluster, metallic iron whisker, mineralogy, ferrous metallurgy.

I. Introduction and Background

IN the past few decades, direct reduction (DR) has become an important new process for ironmaking. About 75% of direct reduced iron (DRI) in the world is produced by the Midrex and HYL shaft furnace processes which use syngas as reducing agent [1]–[3]. However, one of the most serious problems encountered with a gaseous shaft furnace is the sticking among individual iron ore pellets [4]–[7]. This unintentional agglomeration of pellets always makes continuous operation impossible. The sticking phenomenon occurs mostly during metallization of ore and accompanied with fibrous irons [8], [9]. It is influenced by temperature, the type and size of iron ore, the content of gangue, reduction step and addition of hydrogen in the gas mixture. The sticking tendency depends strongly on reduction temperature according to J. Fang [3], [10]. The external shape of the iron ore affected the sticking as well. Spheroid shape was proved to be minor tendency to sticking compared with angular shape [8], [11]. Previous investigations had revealed that the higher the gangue amount in ores the smaller the sticking tendency was. On the other side, ores with higher gangue portion might cause lower melting temperature which could also induce sticking greatly [8], [12], [13]. In the aspect of reducing agent, the pore structure of iron obtained by CO reduction was coarser than that by H2 reduction and the result of small additions of hydrogen was that the fibrous iron growth decreased and stopped if the hydrogen addition increased greatly [8], [14], [15].

The effect of temperature, gas composition and reduction degree on the sticking behavior during reduction of iron ore pellets was examined in [16]. Morphology of sample was analyzed by scanning electron microscope equipped with EDS to reveal the mechanisms of sticking It was found that with increasing temperature the iron precipitation varied. Fibrous iron precipitated on the sticking interface hooked the pellets together at lower temperatures. While at high temperature, sintering of freshly precipitated iron with high activity and surface energy led to the rise of sticking index. Pellets reduced by CO exhibited the highest sticking index for the dense iron layer that precipitated on the interface. Addition of H_2 to reducing gas considerably decreased the sticking index due to the formation of porous and fibrous iron precipitation on the interface, which can be used as an effective inhibition of sticking in iron ore reduction process.

Sticking practically occurred on micro-convexities and edge angles on the surface at lower reduction degree, and then developed connection in large area as edge angles transformed to flat surface with the rise of reduction degree. The precipitation morphology of metallic iron and evolution process of mineralogical structure at gas-solid interface during reduction were studied by in situ observation and thermal analysis to identify the relationships between the precipitation morphology of metallic iron and micro-structure, sticking property [17]. Results indicate that metallic iron is mainly formed as iron whisker with fibrous shape in the Fe_2O_3 reduction under CO atmosphere, and reduction rate is main reason for the difference of this morphology. In the conversion of Fe_2O_3 to Fe_3O_4 to FeO, the volume is changed due to lattice transformation and accompanying with crack and hole. The nucleation and growth of iron whiskers (100% pure iron) proceed in the conversion of FeO-Fe. Therefore, in order to avoid the formation of iron whiskers, the oriented migration of atom iron should be inhibited in the conversion of FeO-Fe.

The initial stages of the wüstite reduction was investigated by Inami et al. [18], [19] through the reduction of dense wüstite samples by CO/CO_2 at 1203, 1273 and 1323K. They found that the reduction started initially very slow and the

M. Bahgat is Staff Scientist, MT – SABIC Technology Center – Jubail Saudi Basic Industries Corporation, P.O Box 11669, Jubail 31961, Saudi Arabia (e-mail: saddikmb@sabic.com).

H. A. Hanafy is Sr. Engineer TP, Metals SBU, Saudi Basic Industries Corporation, Jubail Industrial City 31961, Saudi Arabia (e-mail: hanafiha@sabic.com).

S. Lakdawala is Senior Process Engineer, Saudi Iron and Steel Company, P.O Box 10053, Jubail 31961, Saudi Arabia (e-mail: LakdawalaS@hadeed.sabic.com).

metallic iron not formed but only changing in the wüstite composition which followed by the change in the sample mass. No details are mentioned about this initial stage and its morphology whereas it can be affected by other factors. Then the reduction rate increases with the formation of metallic iron whereas the morphology of formed iron controls the reduction rate after that.

The morphologies of the produced iron during the reduction of dense wüstite samples were also clarified by Hayes et al. [20], [21] using CO/CO_2 or H_2/H_2O gas mixture. Different three types of morphology were observed. Type A porous iron, type B porous wüstite covered with dense iron and type C dense wüstite covered with dense iron. In case of type B a large pits in the wüstite are formed then covered with dense iron while in C no significant surface depressions or pores were observed. The growth of porous nature in type A increase the reaction rate due to allowing the direct contact between gas and wüstite while the reverse take place with type B and C in which the reduction rate is decreased due to the formation of the dense iron layer. Also, it was found that type A takes place due to the breakdown of the dense iron layer that was formed over the wüstite surface and so porous iron is formed. Type B, which is a porous wüstite, covered with dense iron takes place when the chemical reaction rate is high and the difference in iron concentration between the surface and the bulk is high. So, the wüstite decomposed forming instabilities and so large pores are obtained then iron nucleation started and spreads over the surface. Type C takes place when the chemical reaction rate is slow and the difference in iron ion concentration between the sample surface and the bulk is small and so the initial decomposition of the wüstite surface occurs in planar manner leading to a dense wüstite covered with dense iron.

Some investigators [22]-[24] studied the mechanism of metallic iron formation in reduction of wüstite and it was found that the growth of different morphologies iron on wüstite is explained on the basis of C. Wagner's mechanism for the reduction of non-stoichiometric oxides. It takes into account the simultaneous effects of the chemical reaction at the surface and of iron transport in the bulk, which result in an accumulation of iron in the supersaturated wüstite. They stated that the overall reduction process may be divided into three mechanisms. Under pure diffusion control, the site with the lowest critical iron activity thus gives birth to the first metal nucleus and the subsequent growth of this nucleus can take place only via further removal of oxygen around it, since there is no buildup of iron to feed it from the bulk. Diffusion being slow in all directions, so nucleation takes place at many other points independently in a short time until they merge to form a dense layer of iron. Under pure chemical control, in this mechanism, iron is fed to the nucleus down a very steep gradient which substantiates the extreme assumption that the rate of the transport mechanism is much higher than that of further reduction. Growth then takes place without any significant removal of oxygen around the nucleus a condition which leaves it no other possibility than to grow outwards. Under mixed control, the activity of iron at the surface can reach the local critical value at several points over a period of time and several nuclei can appear then the iron built up in the supersaturated zone and the continuing surface reaction. Oxygen being removed on their sides, the nuclei grow radially as well as outwards and assume conical shapes.

The current investigation aims to clarify further the relation between metallic iron whisker growth and iron ore mineralogy to decrease the possibility of cluster formation through, comparative evaluation for the effect of various parameters such as ore type and pellets size.

II. Experimental Work

A. Raw Material

Three different iron ore pellets (A, B, C) were used in the present experiments. High purity (99.99%) H_2, CO and N_2 were used as experimental gas. The reducing gas was a mixture of H_2 and CO with gas ratio about 63/37 respectively to simulate the used Midrex gas.

B. Experimental Procedure

Iron ore pellets were coated with various concentrations of cement suspension and then applied for comparative reducibility test. The apparatus consists of a reduction furnace supported with a system to supply and regulate the gases, a reduction tube of heat resistance steel, a weighing device to determine the oxygen loss at regular intervals and an electrically heated furnace to heat the test portion to the specified temperature. The sample weight used for each reduction test is about 500g in the size range 10.0-12.5 mm. The flow rate of reducing gas during the test period is maintained at about 50 l/min while the temperature is maintained at 995 ^oC. The schematic diagram and visual photo of experimental apparatus used in this study were presented in Figs. 1 and 2 respectively.

The sample is introduced into the chamber. In order to achieve a more uniform gas flow, a two layer bed of porcelain pellets having a size range of 10.0-12.5 mm are placed between the perforated plate and the test portion. The control panel is used to create the desired program. The reduction tube is closed, inserted into the furnace and suspended centrally from the weighing device. The test samples are dried inside the furnace then Nitrogen gas is allowed to pass through the reduction tube at a flow rate of approximately 25 l/min and the heating is commenced. After the mass of the test portion become constant H_2 - CO gas mixture is introduced at a rate of 31.5 and 18.5 l/min respectively. The mass of the test portion is recorded continuously.

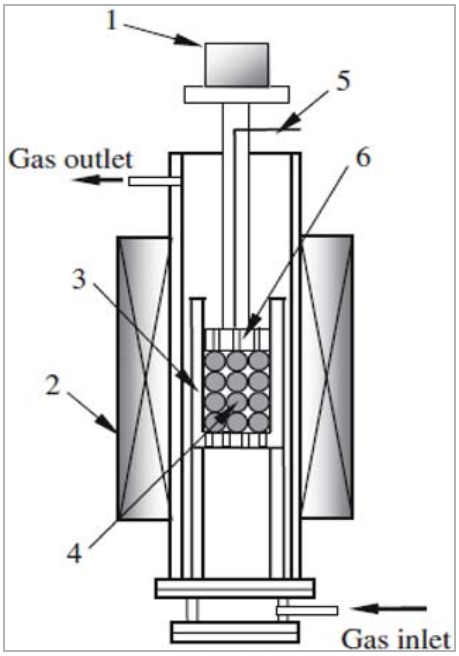

Fig. 1. Schematic diagram of the reduction apparatus
1-Weighting system, 2- Tube furnace, 3- Sample holder, 4- Sample bed in ceramic balls, 5- Thermocouple and 6- Upper grid

Fig. 2. Visual photo of the reduction apparatus

III. Results and Discussion

A. Characterization of Iron Ore Samples

Iron ore pellets samples were characterized with X-ray diffraction analysis (XRD), X-ray fluorescence (XRF) and scanning electron microscope (SEM). The chemical analysis for these ores is shown in Table I. It can be seen that iron oxide (Fe_2O_3) is the major phase with presence of SiO_2, CaO and Al_2O_3 as minor components. For SEM the sample to be examined was fixed into an epoxy resin mould, and then examined under scanning microscope. The SEM photos for the various iron ores (A, B and C) samples are shown in Fig. 3. It was observed that grain coalescence with very low micropores and some macropores took place in a dense structure.

TABLE I
XRF Analysis for Iron Ores A, B & C

Iron Ore (A)		Iron Ore (B)		Iron Ore (C)	
Compound	Conc. %	Compound	Conc. %	Compound	Conc. %
MgO	0.1500	MgO	0.1200	MgO	0.6600
Al2O3	0.3510	Al2O3	0.7360	Al2O3	0.1500
SiO2	1.4400	SiO2	2.1900	SiO2	0.9320
P2O5	0.0720	P2O5	0.0550	P2O5	0.0660
S	0.0240	S	0.0190	S	0.0220
K2O	0.0099	K2O	0.0091	K2O	0.0280
CaO	0.8920	CaO	0.9980	CaO	1.0200
TiO2	0.0437	TiO2	0.0848	TiO2	0.1760
V2O5	0.0094	V2O5	0.0100	V2O5	0.2080
Cr2O3	0.0496	Cr2O3	0.0532	Cr2O3	0.0194
MnO	0.0561	MnO	0.0841	MnO	0.0746
Fe2O3	96.6	Fe2O3	95.5	Fe2O3	96.5
NiO	0.1400	NiO	0.1150	NiO	0.1160

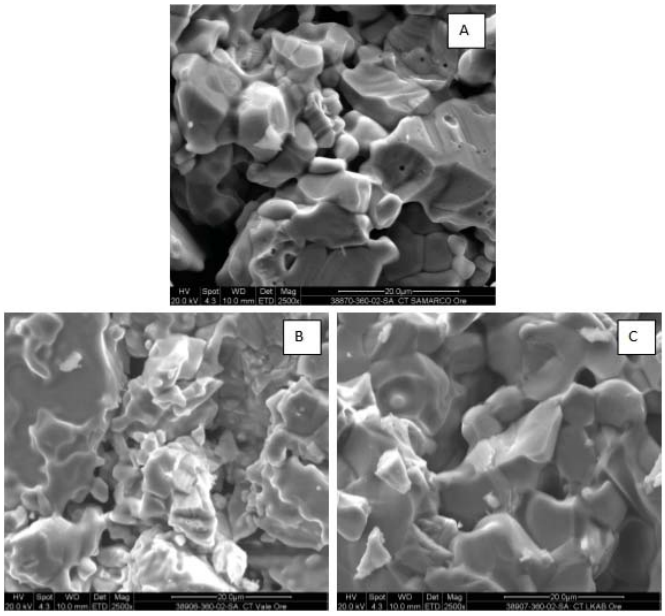

Fig. 3 The SEM photos for iron ores A, B & C

B. Reduction Behavior of Iron Ore Pellets

Using thermo-gravimetric technique, iron ore pellets (A, B and C) were reduced at 985 ºC with H_2/CO gas mixture. The reduced iron ore samples were characterized with X-ray diffraction analysis (XRD), X-ray fluorescence (XRF) and scanning electron microscope (SEM). It can be seen that metallic iron (Fe) is the major phase with presence of SiO_2, CaO and Al_2O_3 as minor components. The influence of pellet size and chemical composition of each ore on the reduction behavior and structural characteristics of the reduced products was studied in order to elucidate the optimum conditions for avoiding the metallic whisker formation.

C. Influence of Pellet Size

The effect of different pellet size +6-12 mm and +12 mm was studied. The reduction curve of iron ore A pellets with different sizes is shown in Fig. 4. It can be seen that the rate of reduction was highest at the early stages and decreased as reduction proceeds till the end of reduction. Also it was

observed that smaller size pellets have higher reduction rate compare to larger one. The morphology of reduced iron ore pellets is shown in Fig. 5. The formed metallic structure is homogenously formed in a very porous structure. On the other hand, larger size pellets have higher tendency for metallic iron whisker formation.

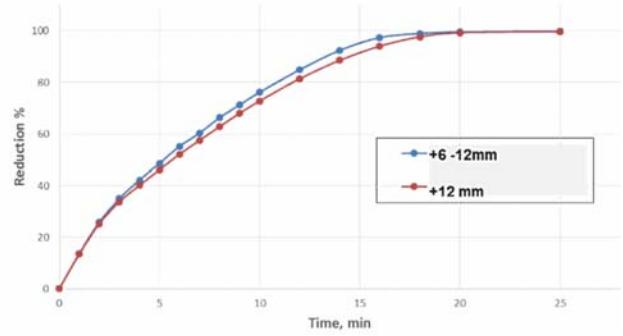

Fig. 4 The reduction curves for different pellet size of iron ore A

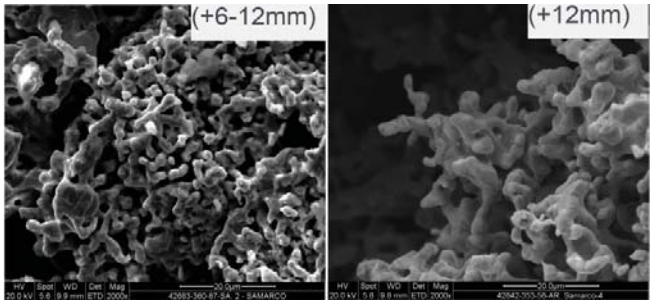

Fig. 5 The SEM micrograph for the outer surface of different pellet size of iron ore A after reduction

The reduction curve of iron ore B pellets with different sizes s shown in Fig. 6. The reduction behavior and formed metallic morphology came similar to ore A as shown in Fig. 7.

The reduction curve of iron ore C pellets with different sizes is shown in Fig. 8. The observed reduction behavior is following ores A and B. Also the morphology of the formed metallic iron structure is similar to the formed structure in ore A and B as shown in Fig. 9.

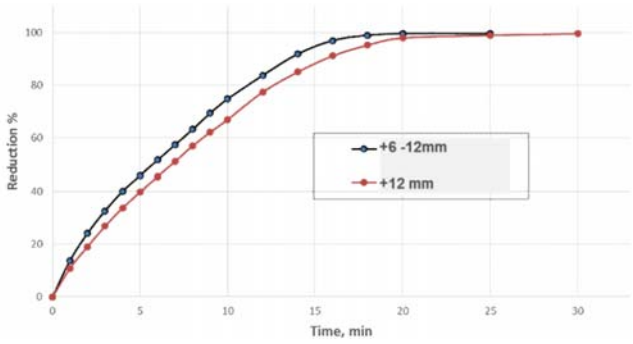

Fig. 6 The reduction curves for different pellet size of iron ore B

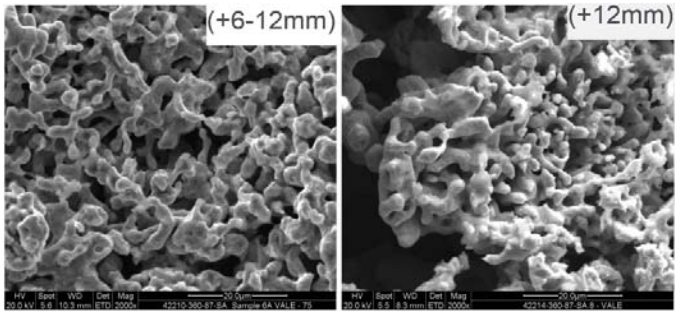

Fig. 7 The SEM micrograph for the outer surface of different pellet size of iron ore B after reduction

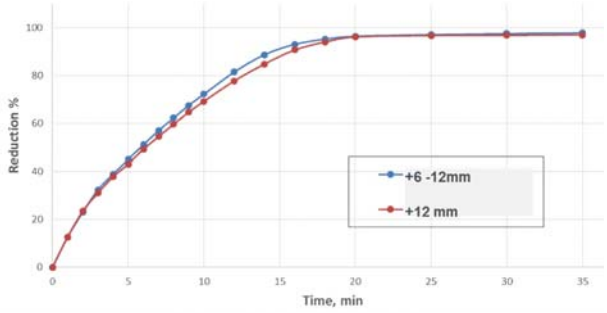

Fig. 8 The reduction curves for different pellet size of iron ore C

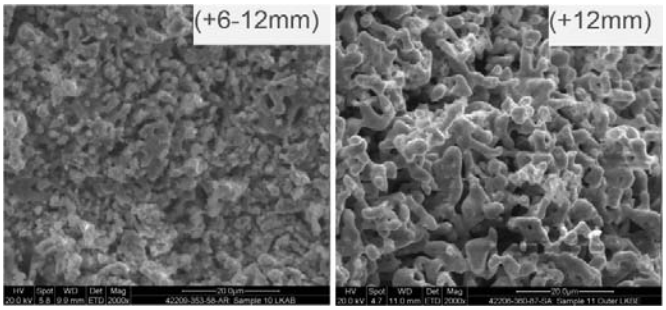

Fig. 9 The SEM micrograph for the outer surface of different pellet size of iron ore C after reduction

D. Influence of Ore Chemical Composition

The effect of chemical composition of each ore was studied. The reduction curves of iron ores A, B and C pellets with similar size (+6 – 12mm) is shown in Fig. 10. For each single reduction curve, the rate of reduction was highest at the early stages and decreased as reduction proceeds till the end of reduction. The reduction rate value came similar for the different samples. However, the iron ore A has relatively higher reduction rate than ore B and ore C has the lowest reduction rate. The SEM micrographs for the outer surface of these reduced iron ore pellets are shown in Fig. 11. It can be seen that the metallic iron is homogenously formed in a very porous structure with presence of large number of micro- and macro-pores. In addition to that iron ore A has relatively has higher tendency for metallic iron whisker formation than ore B and ore C has the lowest tendency.

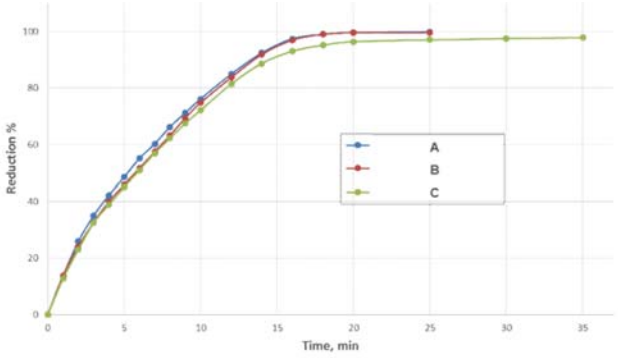

Fig. 10 The reduction curves for different iron ore pellets A, B and C with similar size (+6-12mm)

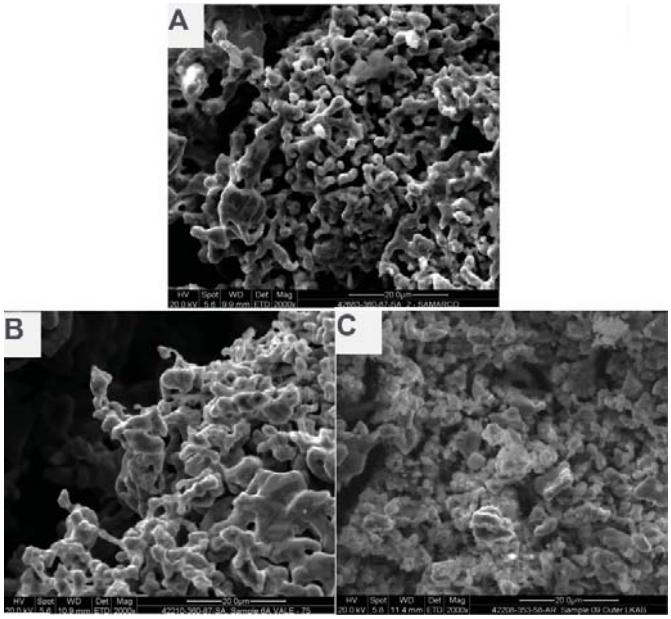

Fig. 11 The SEM micrograph for the outer surface of different iron ore pellets A, B and C with similar size (+6-12mm) after reduction

The reduction curves of iron ores A, B and C pellets with similar size (+12mm) is shown in Fig. 12. The reduction rate increase gradually with increasing reaction time and it was highest at the early stages and decreased as reduction proceeds till the end of reduction. The reduction rate was higher for iron ore A compare to ore B and ore C. The morphology of outer surface is shown in the SEM micrographs Fig. 13.

IV. Conclusions

1) Reducibility increases by decreasing the iron ore pellet's size.
2) Reducibility order according to ore type; Ore A is the highest then ore B and then ore C.
3) Tendency for metallic iron whisker formation (inner/ outer) decreases by decreasing the reduced iron ore pellet's size (faster reducibility decreasing the whisker formation)

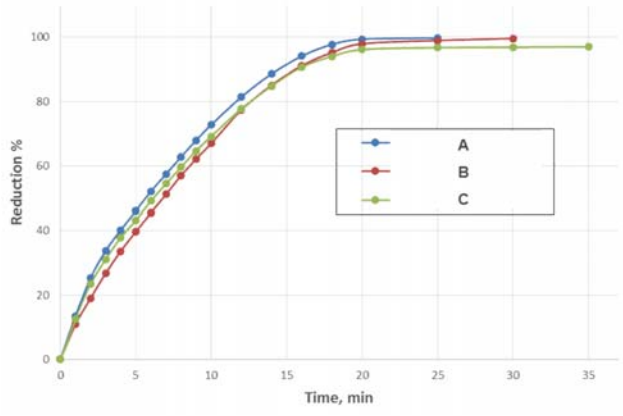

Fig. 12 The reduction curves for different iron ore pellets A, B and C with similar size (+12mm)

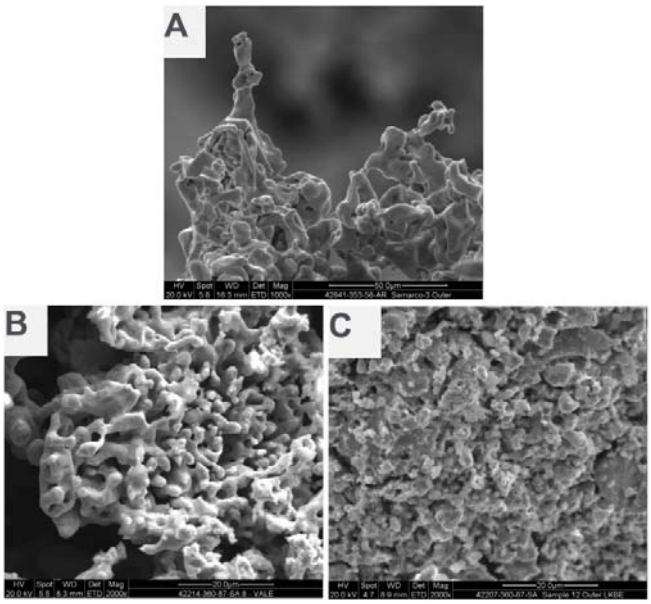

Fig. 13 The SEM micrograph for the outer surface of different iron ore pellets A, B and C with similar size (+12mm) after reduction

4) The order for metallic iron whisker formation according to ore type; Ore A is the highest then ore B and then ore C.
5) The diffusion reaction mechanism is prominent compare to chemical reaction mechanism in ore A than in ore B and C.
6) The comparative porosity and basicity for such ores could be the reason for this behavior (reducibility & whisker formation).

References

[1] H.R. John Kopfle, Direct reduction's role in the world steel industry, Ironmaking and Steelmaking 35 (2008) 254–259.
[2] Midrex technologies, Inc., 2010 world direct reduction statistics, http://www. Midrex.com, 2011.
[3] J. Fang, Theory of Non-Blast Furnace Ironmaking Process, Metallurgical Industry Press, Beijing, 2002.
[4] Ali Basdag, Ali Ihsan Arol, Coating of iron oxide pellets for direct reduction, Scandinavian Journal of Metallurgy 31 (2002) 229–233.

[5] P.L. Hooey, K. Zarins, A. Dahlstedt, H. Annersten, Behaviour of kaolinite coated olivine pellets in blast furnace, Ironmaking and Steelmaking 31 (2004) 333–341.
[6] K.S. Abdel-Halim, M.I. Nasr, A.A. El-Geassy, Developed model for reduction mechanismof iron ore pellets under load, Ironmaking and Steelmaking 38 (2011) 189–196.
[7] P.L.M. Wong, M.J. Kim, H.S. Kim, C.H. Choi, Sticking behaviour in direct reduction of iron ore, Ironmaking and Steelmaking 26 (1999) 53–57.
[8] Shoji Hayashi, Yoshiaki Iguchi, Factors affecting the sticking of fine iron ores during fluidized bed reduction, ISIJ International 32 (1992) 962–971.
[9] M.I.R.K.O. Komatina, Heinrich -W, The sticking problem during direct reduction, Metalurgija (2004) 309–328.
[10] J. Fang, Sticking problem in fluidized bed iron ore reduction, Iron and Steel 26 (1991) 11–15.
[11] Shoji Hayashi, Satoshi Sawai, Yoshiaki Iguchi, Influence of coating oxide and sulfur pressure on sticking during fluidized bed reduction of iron ores, ISIJ International 33 (1993) 1078–1087.
[12] W.L. Malte Bartels, John Nijenhuis, Freek Kapteijn, J. Ruud van Ommen, Agglomeration in fluidized beds at high temperatures: mechanisms, detection and prevention, Progress in Energy and Combustion Science 34 (2008) 633–666.
[13] D.R. Higgins, N.B. Gray, M.R. Davidson, Simulating particle agglomeration in the flash smelting reaction shaft, Minerals Engineering 22 (2009) 1251–1265.
[14] J.F. Gransden, J.S. Sheasby, The sticking of iron ore during reduction by hydrogen in a fluidized bed, Canadian Metallurgical Quarterly 13 (1974) 649–657.
[15] Shoji Hayashi, Sougo Sayama, Yoshiaki Iguchi, Relation between sulfur pressure and sticking of fine iron ores in fluidized bed reduction, ISIJ International 30 (1990) 722–730.
[16] Lingyun Yi, Zhucheng Huang, Tao Jiang, Powder Technology 235 (2013) 1001–1007
[17] Zhao, Z.-L., Tang, H.-Q., Guo, Z.-C., Journal of Iron and Steel Research 24 (11) (2012) , pp. 23-28
[18] T. Inami and K. Suzuki, Tetsu to Hagane, 80 (1994), 699-704.
[19] T. Inami and K. Suzuki, Tetsu to Hagane, 81 (1995), 1037-1042.
[20] D. H. St. John and P. C. Hayes, Met. Trans., 13B (1982), 117-124.
[21] D. H. St. John, S. P. Matthew and P. C. Hayes, Met. Trans., 15B (1984), 701-717.
[22] C. T. Rae and P. C. Hayes, Ind. Tech. Res. Inst., 1(2) (1986), 137-148.
[23] S. P. Matthew, T. R. Cho and P. C. Hayes, Met. Trans., 21B (1990), 733-741.
[24] R. Nicolle and A. Rist, Metallurgical Trensactions B, 10B (1979), 429.